Chapter 8

Synthesis and Characteristics of Carbon Nanofibers/Silicon Composites and Application to Anode Materials of Li Secondary Batteries

Chang-Seop Lee and Yura Hyun

Additional information is available at the end of the chapter

http://dx.doi.org/10.5772/63507

Abstract

Among the various synthesizing technologies of carbon nanofibers (CNFs), chemical vapor deposition (CVD) technology, which uses hydrocarbon gas or carbon monoxide as a carbon source gas and pyrolyzes it to grow CNFs on transition metal catalysts, such as Ni, Fe, and Co, has been regarded as the most inexpensive and convenient method to produce CNFs for industrial use. Experimental variables for CVD are source gas, catalyst layers, temperature, and reaction time. Since the particle size of metal catalysts has an influence on the diameter of CNFs, it is possible to control the diameter of CNFs by varying particle sizes of the metal. As such, it is possible to synthesize CNFs selectively through the selective deposition of catalyst metals. In this study, CNFs were grown by CVD on C-fiber textiles, which had catalysts deposited via electrophoretic deposition. The CNFs were coated with a silica layer via hydrolysis of TEOS (tetraethyl orthosilicate), and the CNFs were oxidized by nitric acid. Due to oxidation, a hydroxyl group was created on the CNFs, which was then able to be used as an activation site for the SiO_2. CNFs and the CNFs/SiO_2 composite can be used in various applications, such as a composite material, electromagnetic wave shielding material, ultrathin display devices, carbon semiconductors, and anode materials of Li secondary batteries. In particular, there is an increasing demand for lightweight, small-scale, and high-capacity batteries for portable electronic devices, such as laptop computers or smart phones, along with the escalating concern of fossil energy depletion. Accordingly, CNFs and CNFs/SiO_2 composites are receiving attention for their use as anode materials of Li secondary batteries, which are eco-friendly, lightweight, and high capacity. Therefore, the physicochemical properties and electrochemical performance data of synthesized CNFs and CNFs/SiO_2 composite are described in this chapter.

Keywords: carbon nanofibers, chemical vapour deposition, silicon composites, anode materials, Li secondary batteries

1. Introduction

Carbon has various types of allotrope (graphite, diamond, carbon nanofibers (CNFs), carbon nanotubes, graphene, etc.) depending on the molecular bonding mode with hybridized bonding of sp, sp^2, and sp^3. **Figure 1** shows a schematic of carbon fibers and tubes of various sizes.

CNFs among various allotropes of carbon are fibrous carbon materials with less than 1 μm thickness and over 90% carbon content and can take various forms, such as herringbone, platelet, and spiral. Such CNFs can be used in various applications, such as a composite material, electromagnetic wave shielding material, ultrathin display devices, carbon semiconductors, and anode materials of secondary batteries. In particular, there is an increasing demand for lightweight, small-scale, and high-capacity batteries for portable electronic devices, such as laptop computers or smart phones, along with the recent concern of fossil energy depletion. Accordingly, CNFs are receiving attention for their potential use as anode materials of Li secondary batteries, which are eco-friendly, lightweight, and high capacity. Secondary batteries can be charged and discharged several times for reuse. Lead and Ni-Cd batteries have been most commonly used prior to the introduction of Li secondary batteries, but they harbor the disadvantages of a memory effect and environmental pollution issues.

Recently, the development of Li secondary batteries received more attention, since they are environmentally safe, with lightweight, small-scale, and high-capacity features required for small IT devices, such as laptop computers or mobile phones [1–17].

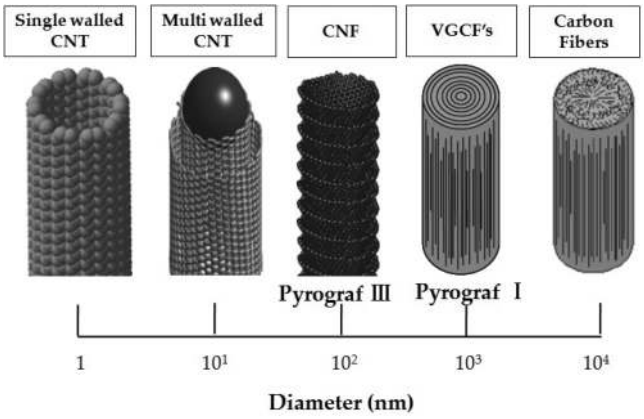

Figure 1. Schematic of carbon fibers and tubes of various types.

1.1. Lithium secondary batteries

Li secondary batteries mainly consist of a cathode, anode, electrolyte, and separator. The anode reversibly intercalates and disintercalates the lithium ions coming from the cathode to allow

http://dx.doi.org/10.5772/63507

electrons to flow through the internal circuit and generate electricity. **Figure 2** shows a schematic diagram showing the principle behind the Li secondary battery.

Studies on the performance enhancement of lithium secondary batteries are mostly concerning the performance improvement of anode materials, including carbon materials and the development of new materials. Since the charging and discharging performance of Li secondary batteries is significantly influenced by the structure of the anode materials for intercalating lithium ions, this study focused on the performance improvement and development of carbon materials as anode materials to allow more Li ions to be inserted. For such anodes, graphite, first developed by Bell Labs in 1981, has been used in most cases. Graphite has the advantage of its crystal structure during charging and discharging, so that its volume does not significantly change; however, it limits the performance of the Li secondary batteries, due to its small maximum theoretical capacity of 372 mAh g^{-1}.

Accordingly, studies are actively conducted to test new carbon-based materials that would allow high-capacity and performance improvement of Li secondary batteries. The CNFs of carbon-based anode materials do not change significantly in their crystal structure during the intercalation and disintercalation process of lithium ions, as in the case of graphite. They are accordingly receiving attention as a new anode material that would allow lithium secondary batteries to provide an excellent lifetime [18–20].

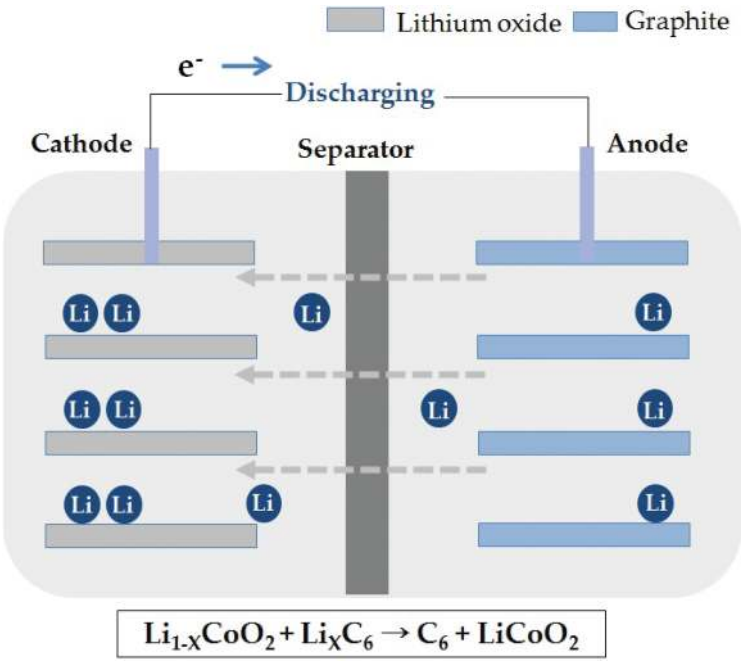

Figure 2. Schematic diagram of the principle of the Li secondary battery.

1.2. CNFs/silicon composites

Silicon is suitable as a high-capacity anode material because of its high maximum theoretical capacity of 4200 mAh g^{-1}; however it is associated with a deteriorating electrical connection due to cracks forming as a result of the nearly 400% volume change during charging and discharging. It also has the problem of deteriorating charging and discharging characteristics by generating a large irreversible capacity. Various studies have been attempted to solve the problems of CNFs and silicon, and a method of synthesizing CNFs/Si composites was presented as one of the solutions [19].

Since CNFs provide a flexible space for the volume expansion of silicon in the process of synthesizing CNFs/Si composite, it has the potential to be a good candidate and as such has been selected as an anode material of Li secondary batteries in order to enhance its performance for use in this study. **Figure 3** shows the grown CNFs on a Si surface which play a role as shrinked springs when the composites are charged.

CNFs were synthesized by using chemical vapor deposition (CVD), and the effects of synthesis conditions, such as synthesis temperature and the concentration ratio of catalysts on the growth of CNFs, were studied. CNFs/Si composites were synthesized based on these CNFs, and the physiochemical characteristics of CNFs/Si composites and the electrochemical characteristics as anode materials of Li secondary batteries were also investigated [9, 18–22].

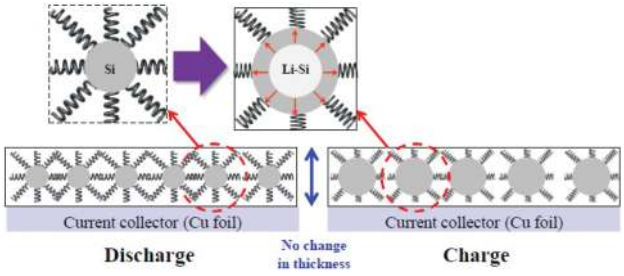

Figure 3. Schematic diagram showing the buffering principle of CNFs/Si composites.

2. Synthesis of CNFs on electroplated Fe/C-fiber textiles

2.1. Experimental process

2.1.1. Oxidation

C-fiber textiles (SGL Carbon Group) were put into 60% nitric acid and heated at 80°C for 30 min under reflux to form OH groups on the surface of C-fiber textiles. After the completion of oxidation, the oxidized C-fiber textiles were cleaned and stored in distilled water, without drying in an oven, in order to keep the OH groups attached to the surface [4, 7, 17].

http://dx.doi.org/10.5772/63507

2.1.2. Deposition of Fe catalyst

For the deposition of a Fe catalyst, $Fe(NO_3)_3 \bullet 9H_2O$ as a precursor was first dissolved in distilled water, and then the C-fiber textiles were immersed in the solution. The pH of the solution was lowered to 1.00 with nitric acid, and the solution was heated to 90°C. The ratio of C-fiber textiles and the amount of Fe in the solution was controlled as an experimental variable. Afterward, hydrolysis was carried out by slow dropping of 1 M urea solution.

It is known that $Fe(OH)_3$ is formed by deposition-precipitation on the surface of oxidized C-fiber textiles, through the reaction of OH groups. For comparison, deposition of ferrous particles on the oxidized C-fiber textiles was carried out, by dipping the substrate into the solution, after the hydrolysis by urea was complete. The specimen was cleaned by distilled water, after completion of the deposition process, and dried for 24 hours at 80°C [4, 7, 17].

2.1.3. Reduction

A reduction step was applied in order to convert iron hydroxides and oxides attached to the surface of C-fiber textiles into elemental iron using a tube furnace. Hydrogen balanced with nitrogen gas was used for the reduction process, and the flux of the reaction gas was controlled by an electronic mass flow controller (MFC). The reactor temperature was increased by 10°C/min up to 600°C in pure N_2 atmosphere. Once the temperature reached 600°C, N_2 gas balanced with 20% H_2 gas was flowed into the reactor for 3 hours to carry out the reduction process [4, 7, 17].

2.1.4. Growth of CNFs

CNFs were grown on C-fiber textiles by CVD in a horizontal quartz tube reaction apparatus after completion of the reduction process. The flux of reaction gas was controlled by an electronic MFC, and ethylene gas (C_2H_4) was used to grow the CNFs as a carbon source. Hydrogen gas was used to eliminate the remaining hydroxyl group after the reduction process, while nitrogen was used to stabilize the reaction.

The prepared metal catalyst was evenly spread on a quartz boat, which was placed into the reactor under nitrogen atmosphere, and the reactor temperature was increased by 10°C/min. Once the temperature reached 700°C, it was maintained for 30 min. N_2 gas balanced with 20% H_2 gas was flowed into the reactor, and then 20% ethylene balanced with N_2 gas was flowed into the reactor for 5 hours. After the completion of the reaction, the temperature was lowered to room temperature in N_2 atmosphere [4, 7, 17].

2.2. Physicochemical properties of the grown CNFs

2.2.1. Scanning Electron Microscope (SEM)

Figures 4 and **5** show the shape of the CNFs grown on the C-fiber textiles by the CVD method, as taken by SEM, with 100,000× magnification. It was found that the diameters of CNFs increased with decreasing a Fe/C ratio. The diameters of CNFs grew up to 40–60 nm when the

weight ratio of C-fiber textiles to Fe was 1:30, whereas CNFs grew up to 30–55 nm in diameter when the ratio was 1:70.

In contrast, it was observed that CNFs scarcely grew in the samples prepared by the dip-coating method if the ratio of C-fiber textiles to Fe reached 1:70; instead they started to cohere during the growth process. It is assumed that too many Fe catalyst particles were present on the surface of the C-fiber textiles, which interferes with the growth of CNFs. CNFs of 40–60 nm in diameter grew when the ratio was 1:10, while the thinnest and the most even CNFs, of 25–30 nm in diameter, grew when the ratio was 1:30 [4, 7, 17].

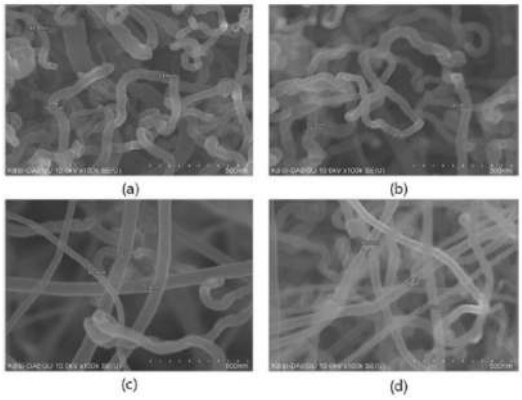

Figure 4. CNFs grown on C-fiber textiles, under the CVD method. (a) 1 g C-fiber textile, 10 g Fe(III) weight ratio; (b) 1 g C-fiber textile, 30 g Fe(III) weight ratio; (c) 1 g C-fiber textile, 50 g Fe(III) weight ratio; and (d) 1 g C-fiber textile, 70 g Fe(III) weight ratio.

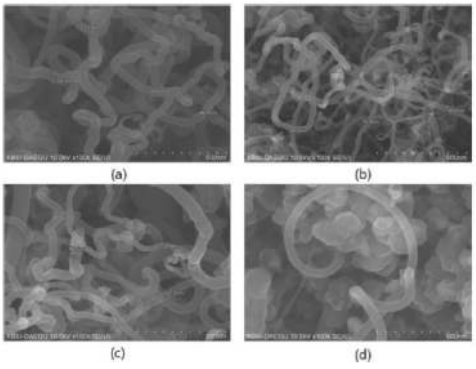

Figure 5. Shapes of CNFs, after the CVD process, when the dip-coating time was 30 min. (a) 1 g C-fiber textile, 10 g Fe(III) weight ratio; (b) 1 g C-fiber textile, 30 g Fe(III) weight ratio; (c) 1 g C-fiber textile, 50 g Fe(III) weight ratio; and (d) 1 g C-fiber textile, 70 g Fe(III) weight ratio.

http://dx.doi.org/10.5772/63507

2.2.2. X-ray Diffraction (XRD)

XRD patterns were taken in order to analyze how the crystalline structure of the samples change according to the different processes, and the results are shown in **Figure 6**. After the deposition process, iron oxide phases of different stoichiometry were found. It is known that $Fe(OH)_3$ present on the sample surface after precipitation-deposition transforms into iron oxide during the drying process, and then Fe particles of cubic crystalline structure remained after reduction.

The graphite peaks in the raw material mainly belong to the graphite flakes, which are present in the C-fiber textile. The peak broadening, which can be observed for the samples after CVD, can be attributed to the presence of CNFs [4, 7, 17].

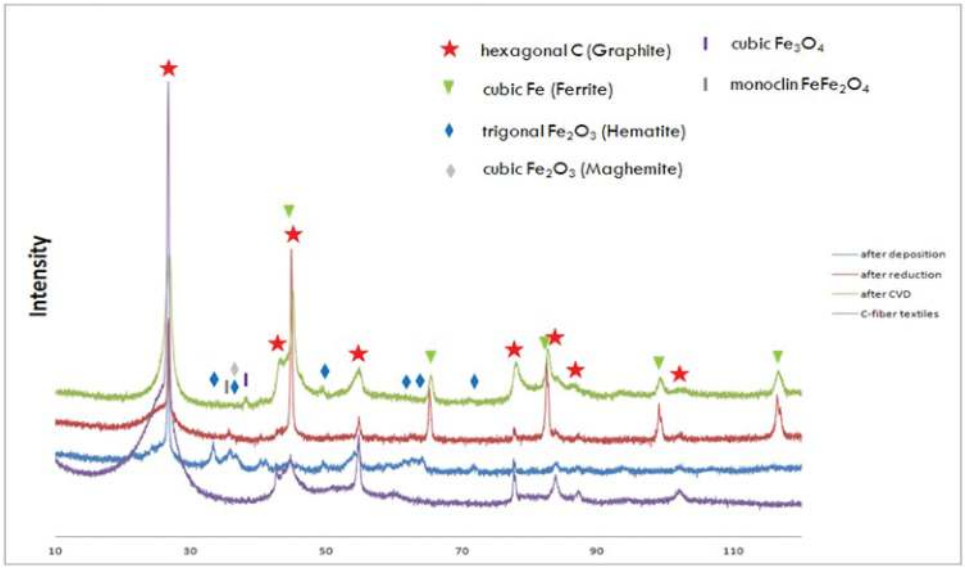

Figure 6. XRD pattern of sample according to changes in the experimental process.

2.2.3. X-ray Photoelectron Spectroscopy (XPS)

XPS analysis was carried out in order to analyze the binding energies of C, Fe, and oxygen. Measurements were performed for the sample where the CNFs (C:Fe 1:30, 30 min dip coating) were grown as uniformly as possible. **Figure 7** shows the XPS analysis result after the growth of CNFs. The binding energy of the Fe catalyst particles deposited to CNFs, which were grown on the surface, did not appear on the XPS spectrum, while the binding energies of C and oxygen appeared on the spectra [4, 7, 17].

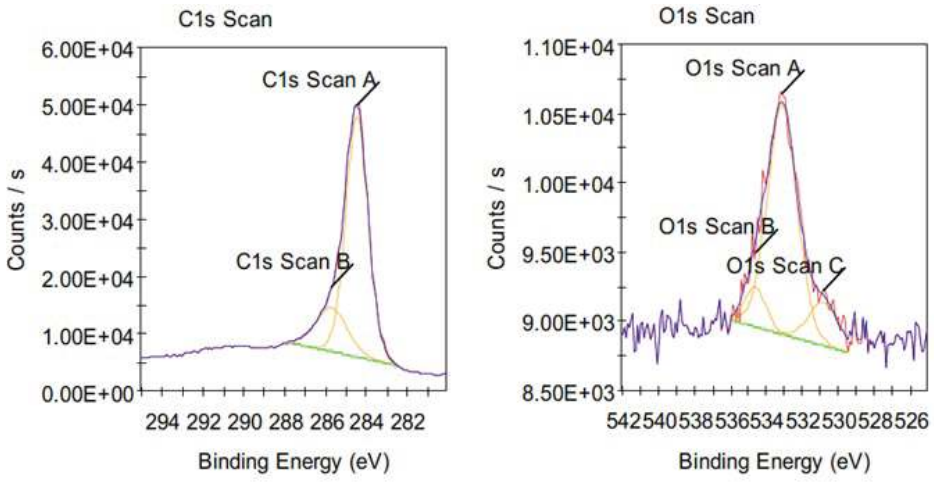

Name	Binding Energy(eV)	Analysis
C1s Scan A	284.46	Graphite C
C1s Scan B	285.7	C-H combination
O1s Scan A	534.63	C-O combination
O1s Scan B	533.13	C=O combination
O1s Scan C	530.81	Fe_2O_3 combination

Figure 7. XPS results of CNFs grown on C-fiber textiles.

2.2.4. Thermogravimetry/Differential Thermal Analysis (TG/DTA)

Figure 8 shows TG/DTA thermograms for the CNF grown samples. After the Fe catalyst was deposited (a) by the deposition-precipitation method or (b) by the dip-coating method, with the same C:Fe ratio of 1:30, analysis was performed on the samples in which CNFs were grown. The TG/DTA curves showed similar tendencies when the experiment was conducted by both methods.

As can be seen in **Figure 8**, the decrease of TGA thermogram ranges from 490°C to 750°C, which resulted from the oxidation of CNFs and C-fiber textiles composing the sample. As for the DTA thermogram, exothermic peaks were found in both samples near 600°C, 690°C, and 850°C. The exothermic peak near 600°C appearing at the beginning of the DTA thermogram is deemed as oxidation reaction to carbon of CNFs; and meantime, exothermic peaks appear-

http://dx.doi.org/10.5772/63507

ing in higher temperature of near 690°C and 850°C are deemed as peaks showing the oxidation reaction of C-fiber and graphite composing C-fiber textiles, which were used as substrate [4, 7, 17].

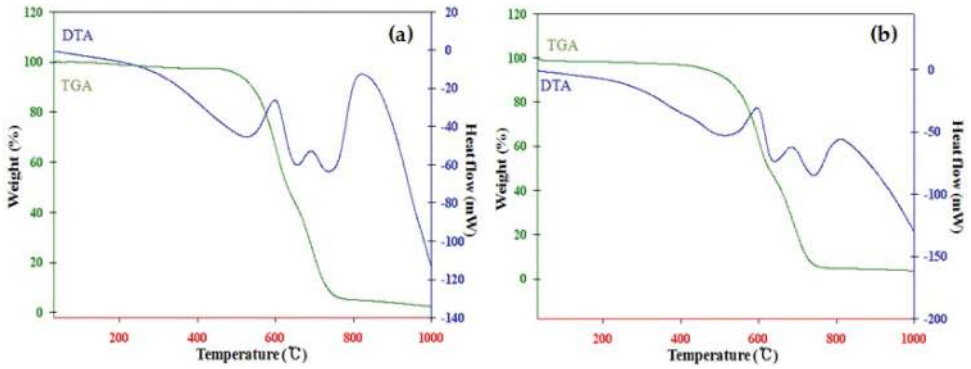

Figure 8. TG/DTA thermograms of CNFs grown on C-fiber textiles by the two different deposition methods: (a) deposition-precipitation method and (b) dip-coating method.

2.2.5. Raman

After CNFs had been synthesized in the CVD method, Raman analysis was performed in order to investigate the characteristics of C— bonding, and the results are presented in **Figure 9**. After Fe catalysts were deposited on CNFs, they were grown on C-fiber textiles by the deposition-precipitation method or dip-coating method with a C:Fe ratio of 1:30. No differences were discovered in the patterns of Raman spectrum by the Fe catalyst deposition method; however the intensity value was relatively larger when the dip-coating method was used, when compared to the deposition-precipitation method.

As seen in **Figure 9**, a D band appeared around 1332 cm^{-1}, a G band around 1582 cm^{-1}, and a 2D band around 2700 cm^{-1}; and the intensity and $R = (I_D/I_G)$ values of the D band, G band, and 2D band appear in the respective spectra. When CNFs were grown after the deposition of Fe catalyst in the two different methods, the respective R values were 0.64 under deposition-precipitation, while they were 0.73 under the dip-coating method. As such, it is known that CNFs grow better, if and when the Fe catalyst is deposited by dip-coating, and then CNFs are grown. Meanwhile, a 2D band appeared in both samples, which means that not only pure CNFs carbon grow but also multiwalled carbon nanotubes (MWCNTs) partially grow together, when CNFs are grown by both the deposition-precipitation and dip-coating methods [4, 7, 17].

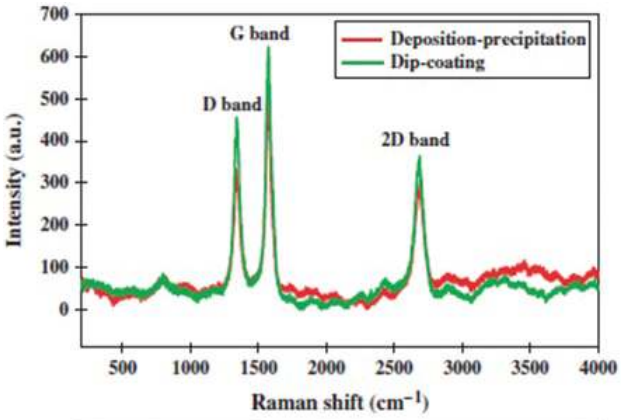

Deposition method of Fe catalyst	*D* band (intensity a.u.)	*G* band (intensity a.u.)	2*D* band (intensity a.u.)	*R* (I_D/I_G)
Deposition-precipitation	323	507	283	0.64
Dip-coating	455	620	364	0.73

Figure 9. The Raman spectra of CNFs grown on C-fiber textiles by the two different deposition methods.

3. Synthesis of CNFs and CNFs/SiO_2 composite on electroplated Co-Ni/C-fiber textiles

3.1. Experimental process

3.1.1. Deposition of Co-Ni catalysts on C-fiber textiles

Using the electrophoretic method, Co-Ni catalysts were deposited on C-fiber textiles. Carbon electrodes and carbon sheets were used as the anode and cathode, respectively, while a mixture of cobalt nitrate and nickel nitrate was used as the electrolyte. To analyze the characteristics of the CNFs according to their cobalt and nickel contents, cobalt nitrate and nickel nitrate, with the weight ratio of 6:4 and 8:2, were used as the electrolyte for the deposition of Co-Ni catalysts by applying 0.04–0.05 A of current for 5 min [4, 7, 17, 18, 22].

3.1.2. Reduction of catalysts and synthesis of CNFs

After placing the C-fiber textiles with deposited catalysts into a furnace, the temperature was increased by 12°C/min up to 700°C in N_2 atmosphere. While maintaining the temperature at 700°C, H_2 gas was flowed into the furnace for 1 hour for the reduction of the catalysts.

http://dx.doi.org/10.5772/63507

Using CVD, CNFs were synthesized to electroplated Co-Ni/C-fiber textiles. Ethylene gas, as the C source, was flowed into the furnace for an hour at 700°C, during which reduction was completed. After the completion of the reaction, the temperature was lowered to room temperature in N_2 atmosphere [4, 7, 17, 18, 22].

3.1.3. Synthesis of the CNFs/SiO_2 composite

For the silica coating, a hydroxyl group was attached to the surface of the CNFs as an anchor group and oxidized for 30 min in 80°C nitric acid. Using the sol-gel process, SiO_2 was applied as a coating through the hydrolysis of tetraethyl orthosilicate (TEOS) on the surface of the reduced CNFs. TEOS was hydrolyzed by dissolving hydrochloric acid and distilled water with ethanol and stirred for 6 hours at room temperature. After soaking the CNFs/C-fiber textiles in this solution and adding ammonia solution for gelation, the solution was stirred for 12 hours and SiO_2 was coated on the surface of the CNFs [4, 7, 17, 18, 22].

3.1.4. Fabrication of coin cell

To investigate the electrochemical characteristics of the CNFs and the CNFs/SiO_2 composite, a coin cell was fabricated. For the working electrode, the CNFs and CNFs/SiO_2 deposited on C-fiber textiles were used without a binder, Li metal was used for the counter electrode, and polyethylene was used for the separator. For the electrolyte, $LiPF_6$ was dissolved in ethylene carbonate (EC) and diethyl carbonate (DEC) (1:1 vol.%) for a mixed solution. The coin cell was fabricated in a glove box filled with Ar gas [4, 7, 17, 18, 22].

3.2. Characterization of the CNFs/SiO_2 composite

3.2.1. Scanning Electron Microscope (SEM)

Figure 10 shows the SEM images of CNFs synthesized according to the Co-Ni ratio. In both samples, CNFs in a curved form with a uniform diameter were synthesized. With a Co-Ni ratio of 8:2, 40 nm CNFs were synthesized, while 30 nm CNFs were synthesized with a ratio of 6:4 [22].

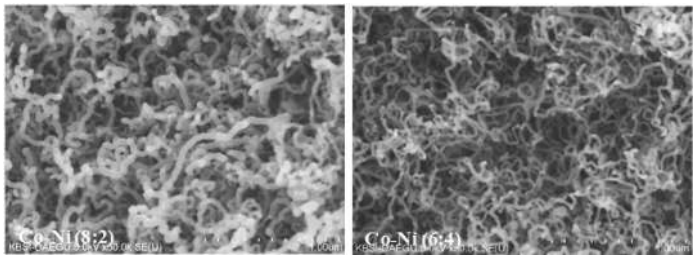

Figure 10. SEM images of CNFs grown on Co-Ni/C-fiber textiles.

3.2.2. X-ray Photoelectron Spectroscopy (XPS)

Figure 11 shows the XPS spectra of CNFs that were synthesized using Co-Ni catalysts. With Co-Ni ratios of 8:2 and 6:4, a C═C (sp^2) bond, C—C (sp^3) bond, —C═O bond, and —COO bond were observed around 285, 286, 288, and 292 eV, respectively. It was found that the catalyst ratio did not affect the binding energy of CNFs as the same C-binding energy was observed with both catalyst ratios.

Figure 12 shows the XPS spectra of the as-synthesized CNFs/SiO_2 composite. Around the binding energy of 103–105 eV for silicon, SiO_2 and SiO were identified. Considering that the intensity of SiO_2 bonding is higher than that of SiO bonding in larger areas, the coated layer on the surface of CNFs consisted mostly of SiO_2 [22].

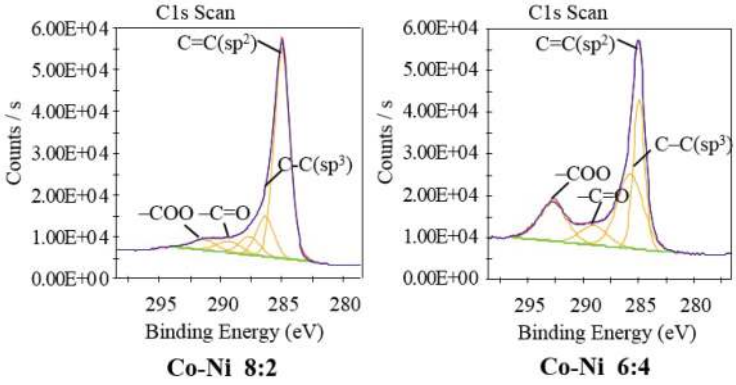

Figure 11. XPS spectra of CNFs grown on Co-Ni/C-fiber textiles.

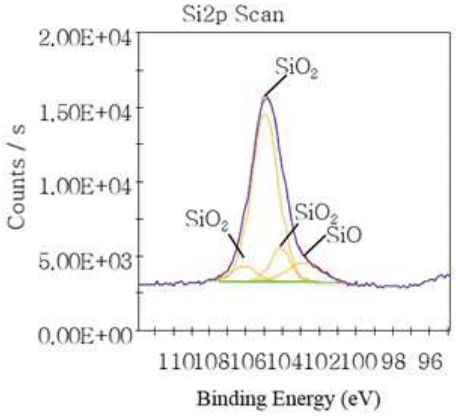

Figure 12. XPS spectra of CNFs/SiO_2 composite.

http://dx.doi.org/10.5772/63507

3.2.3. Raman

Figure 13 shows the Raman spectra of CNFs according to the Co-Ni ratios. Around 1590 cm^{-1}, a G band indicating a C═C (sp^2) bond was observed, while a D band indicating a C—C (sp^3) bond was observed around 1350 cm^{-1}. Considering that the intensity ratio of the D band and B band at both ratios was close to 1, it was determined that CNFs were synthesized with a 1:1 ratio of sp^2 bonds and sp^3 bonds. The intensity of CNFs synthesized at the Co-Ni ratio of 8:2 was higher than that of CNFs synthesized at a 6:4 ratio. Accordingly, this showed that CNFs synthesized at the Co-Ni ratio of 8:2 had higher crystallizability [22].

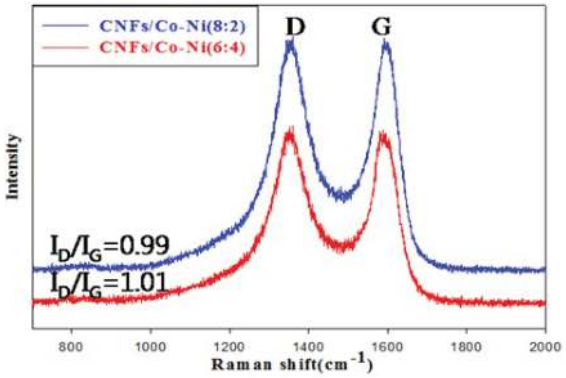

Figure 13. Raman spectra of CNFs grown on Co-Ni/C-fiber textiles.

3.2.4. Transmission electron microscopy (TEM)

To observe the layer of silica coated on the surface of the CNFs, TEM images were examined and are shown in **Figure 14**. For the CNFs coated with silica, CNFs synthesized at the Co-Ni ratio of 8:2 with relatively high crystallizability were used. A layer of silica at a thickness of about 10 nm was coated evenly on the surface of the CNFs in a hollow form with about 8 nm center diameter [22].

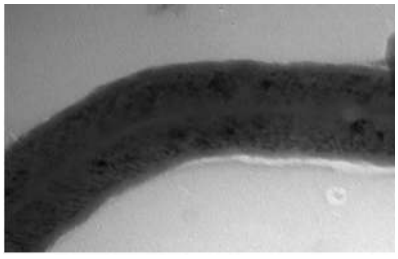

Figure 14. TEM image of SiO_2-coated CNF composite.

3.2.5. Cycle performance

The discharge capacities of C-fiber textiles, CNFs, and CNFs/SiO_2 composite were measured and are shown in **Figure 15**. The respective initial discharge capacities of the CNFs synthesized with the Co-Ni ratios of 8:2 and 6:4 were 258 and 234 mAh g^{-1}, respectively, thereby showing higher results than that of C-fiber textiles with the initial discharge capacity of 190 mAh g^{-1} and a high retention rate of 95%. The CNFs/SiO_2 composite showed the highest initial discharge capacity of 1468 mAh g^{-1} with the retention rate of 47% [22].

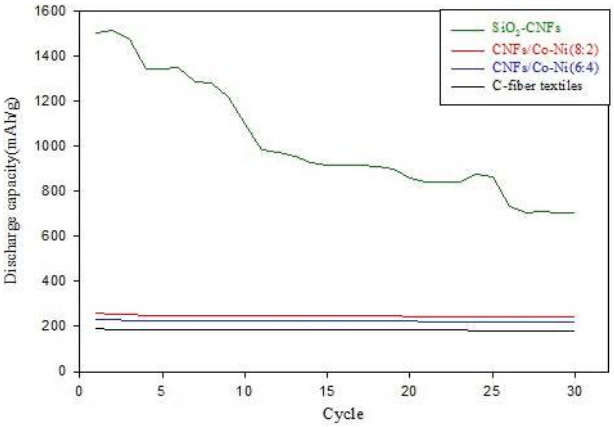

	C-fiber textiles	CNFs/ Co-Ni(8:2)	CNFs/ Co-Ni(6:4)	SiO_2-CNFs
Discharge capacity at 1st cycle	190	258	234	1468
Discharge capacity at 30th cycle	183	244	220	705
Retention rate (%)	96	95	94	47

Figure 15. Discharge capacities and retention rates of C-fiber textiles, CNF/Co-Ni and CNF/SiO_2 composites.

4. Conclusions

Based on the catalysts deposited using the electrophoretic method, CNFs were synthesized on the surface of C-fiber textiles through CVD. Upon hydrolysis of TEOS, silica was coated on the surface of CNFs to synthesize the CNFs/SiO_2 composite. The characteristics of the as-synthesized CNFs and CNFs/SiO_2 composite were analyzed through various spectroscopic methods. Upon fabricating a coin-type half-cell without a binder for the as-synthesized sample, its cycle performance when used as an anode material in Li secondary batteries was investigated. Based on the results, the following conclusions were deduced [22].

1. When the CNFs grew, after deposition of the Fe catalyst using the deposition-precipitation method, the diameters grew up to 40–60 nm and 30–55 nm, when weight ratios of C:Fe were 1:30 and 1:50, respectively.
2. When the CNFs grew, after deposition of Fe catalyst using the dip-coating method, the diameters grew up to 40–60 nm and 25–30 nm, when the weight ratios of C:Fe were 1:10 and 1:30, respectively [4, 7, 17].
3. With Co-Ni ratios of 8:2 and 6:4, CNFs with diameters of 40 and 30 nm were synthesized, respectively [22].
4. The Raman analysis results confirmed that CNFs with a 1:1 ratio of C sp^2 bonds and sp^3 bonds were synthesized when Co-Ni catalysts were used. When the Co-Ni ratio was 8:2, CNFs with higher crystallizability were synthesized compared to that synthesized with a ratio of 6:4 [22].
5. The discharge capacity of the CNFs synthesized on the surface of the C-fiber textiles was 230–260 mAh g^{-1}, about 35% higher than that of pure C-fiber textiles, with a high retention rate of 95% [22].
6. CNFs/SiO_2 composites showed the highest discharge capacity of 1468 mAh g^{-1} with a retention rate of 47% [22].

Acknowledgements

This research was financially supported by the Ministry of Education, Science Technology (MEST) and National Research Foundation of Korea (NRF) through the Human Resource Training Project for Regional Innovation (No. 2015035858).

Author details

Chang-Seop Lee* and Yura Hyun

*Address all correspondence to: surfkm@kmu.ac.kr

Department of Chemistry, Keimyung University, Daegu, South Korea

References

[1] Kenneth B. K. Teo Charanjeet Singh, Manish Chhowalla, Willam I. Milne. Catalytic Synthesis of Carbon Nanotubes and Nanofibers. In: H. S. Nalwa, editor. Encyclope-

dia of Nanoscience and Nanotechnology. 10th ed. USA: American Scientific Publishers; 2003. p. 1–22.

[2] Yoong-Ahm Kim, Takuya Hayashi, Satoru Naokawa, Takashi Yanagisawa, Morinobu Endo. Comparative Study of Herringbone and Stacked-cup Carbon Nanofibers. Carbon. 2005;43:3005–3008. DOI: 10.1016/j.carbon.2005.06.037

[3] Eunyi Jang, Heai-Ku Park, Chang-Seop Lee. Synthesis and Application of Si/Carbon Nanofiber Composites Based on Ni and Mo Catalysts for Anode Material of Lithium Secondary Batteries. Journal of Nanoscience and Nanotechnology. Forthcoming. DOI: 10.1166/jnn.2016.12229

[4] Sang-Won Lee, Chang-Seop Lee. Electrophoretic Deposition of Iron Catalyst on C-Fiber Textiles for the Growth of Carbon Nanofibers. Journal of Nanoscience and Nanotechnology. 2014;14:8619–8625. DOI: 10.1166/jnn.2014.9960

[5] Yura Hyun, Eun-Sil Park, Karina Mees, Ho-Seon Park, Monika Willert-Porada, Chang-Seop Lee. Synthesis and Characterization of Carbon Nanofibers on Transition Metal Catalysts by Chemical Vapor Deposition. Journal of Nanoscience and Nanotechnology. 2015;15:7293–7304. DOI: 10.1166/jnn.2015.10588

[6] Eun-Sil Park, Jong-Won Kim, Chang-Seop Lee. Synthesis and Characterization of Carbon nanofibers on Co and Cu Catalysts by Chemical Vapor Deposition. Bulletin of the Korean Chemical Society. 2014;35(6):1687–1691. DOI: 10.5012/bkcs.2014.35.6.1687

[7] Sang-Won Lee, Chang-Seop Lee. Growth and Characterization of Carbon Nanofibers on Fe/C-Fiber Textiles Coated by Deposition–Precipitation and Dip-Coating. Journal of Nanoscience and Nanotechnology. 2015;15:7317–7326. DOI: 10.1166/jnn.2015.10585

[8] Eunyi Jang, Heai-Ku Park, Jong-Ha Choi, Chang-Seop Lee. Synthesis and Characterization of Carbon Nanofibers Grown on Ni and Mo Catalysts by Chemical Vapor Deposition. Bulletin of the Korean Chemical Society. 2015;36(5):1452–1459. DOI: 10.1002/bkcs.10285

[9] Yura Hyun, Jin-Yeong Choi, Heai-Ku Park, Jae Young Bae, Chang-Seop Lee. Synthesis and Electrochemical performance of Mesoporous SiO_2-Carbon nanofibers composite as anode materials for lithium secondary batteries. Materials Research Bulletin. Forthcoming. DOI:10.1016/j.materresbull.2016.03.006

[10] Xiaojiao Li, Chuncheng Hao, Qingquan Lei. Growth of Carbon Nanofibers Catalyzed by Silica-coated Copper Nanoparticles. Materials Research Bulletin. 2012;47:352–355. DOI: 10.1016/j.materresbull.2011.11.013

[11] Kyung Ho Park, Soonil Lee, Ken Ha Koh. Growth and High Current Field Emission of Carbon Nanofiber Films with Electroplated Ni Catalyst. Diamond and Related Materials. 2005;14(11–12):2094–2098. DOI: 10.1016/j.diamond.2005.06.013

[12] Martijn K. van der Lee, A. Jos van Dillen, John W. Geus, Krijn P. de Jong, Johannes H. Bitter. Catalytic Growth of Macroscopic Carbon Nanofiber Bodies with High Bulk

Density and High Mechanical Strength. Carbon 2006;44(4):629–637. DOI: 10.1016/j.carbon.2005.09.031

[13] Young Joon Yoon, Hong Koo Baik. Catalytic Growth Mechanism of Carbon Nanofibers Through Chemical Vapor Deposition. Diamond and Related Materials. 2001;10(3–7):1214–1217. DOI: 10.1016/S0925-9635(00)00585-9

[14] Jae-Seok Lim, Seong-Young Lee, Sei-Min Park, Myung-Soo Kim. Preparation of Carbon Nanofibers by Catalytic CVD and Their Purification. Carbon Letters. 2005;6(1):31–40.

[15] Taeyun Kim, Karina Mees, Ho-Seon Park, Monika Willert-Porada, Chang-Seop Lee. Growth of Carbon Nanofibers Using Resol-type Phenolic Resin and Cobalt(II) Catalyst. Journal of Nanoscience and Nanotechnology. 2013;13(11):7337–7348. DOI: 10.1166/jnn.2013.7852

[16] Yura Hyun, Haesik Kim, Chang-Seop Lee. Synthesis of Carbon Nanofibers on Iron and Copper Catalysts by Chemical Vapor Deposition. Advanced Materials Research. 2013;750–752:265–275. DOI: 10.4028/www.scientific.net/AMR.750-752.265

[17] Sang-Won Lee, Karina Mees, Ho-Seon Park, Monika Willert-Porada, Chang-Seop Lee. Synthesis of Carbon Nanofibers on C-Fiber Textiles by Thermal CVD Using Fe Catalyst. Advanced Materials Research. 2013;750–752:280–292. DOI: 10.4028/www.scientific.net/AMR.750-752.280

[18] Ki-Mok Nam, Heai-Ku Park, Chang-Seop Lee. Synthesis and Electrochemical Properties of Carbon Nanofibers and SiO_2/Carbon Nanofiber Composite on Ni–Cu/C-Fiber Textiles. Journal of Nanoscience and Nanotechnology. 2015;15:8989–8995. DOI: 10.1166/jnn.2015.11555

[19] Eun-Sil Park, Heai-Ku Park, Ho-Seon Park, Chang-Seop Lee. Synthesis and Electrochemical Properties of CNFs–Si Composites as an Anode Material for Li Secondary Batteries. Journal of Nanoscience and Nanotechnology. 2015;15:8961–8970. DOI: 10.1166/jnn.2015.11554

[20] Yura Hyun, Heai-Ku Park, Ho-Seon Park, Chang-Seop Lee. Characteristics and Electrochemical Performance of Si-Carbon Nanofibers Composite as Anode Material for Binder-Free Lithium Secondary Batteries. Journal of Nanoscience and Nanotechnology. 2015;15:8951–8960. DOI: 10.1166/jnn.2015.11553

[21] Eun-Sil Park, Jong-Ha Choi, Chang-Seop Lee. Synthesis and Characterization of Vapor-grown Si/CNF and Si/PC/CNF Composites Based on Co–Cu Catalysts. Bulletin of the Korean Chemical Society. 2015;36(5):1366–1372. DOI: 10.1002/bkcs.10262

[22] Kun-Ho Jang, Sang-Hoon Lee, Yujin Han, Seong-Ho Yoon, Chang-Seop Lee. Synthesis and Characteristics of Silica-coated Carbon Nanofibers on Electroplated Co–Ni/C-fiber Textiles. Journal of Nanoscience and Nanotechnology. Forthcoming.